

Feasibility analysis of ensemble sensitivity computation in turbulent flows

Nisha Chandramoorthy* and Pablo Fernandez†
Massachusetts Institute of Technology, Cambridge, MA, 02139, USA

Chaitanya Talnikar‡
NVIDIA Corporation, Santa Clara, CA, 95051, USA

Qiqi Wang§
Massachusetts Institute of Technology, Cambridge, MA, 02139, USA

In chaotic systems, such as turbulent flows, the solutions to tangent and adjoint equations exhibit an unbounded growth in their norms. This behavior renders the instantaneous tangent and adjoint solutions unusable for sensitivity analysis. The Lea-Allen-Haine ensemble sensitivity (ES) estimates provide a way of computing meaningful sensitivities in chaotic systems by utilizing tangent/adjoint solutions over short trajectories. In this paper, we analyze the feasibility of ES computations under optimistic mathematical assumptions on the flow dynamics. Furthermore, we estimate upper bounds on the rate of convergence of the ES method in numerical simulations of turbulent flow. Even at the optimistic upper bound, the ES method is computationally intractable in each of the numerical examples considered.

Nomenclature

ES	Ensemble Sensitivity
τ	trajectory length for ES computation
N	number of i.i.d samples used in ES computation
$\theta_{\tau, N}$	ES estimator
	Superscripts T, A and FD stand for tangent, adjoint and finite difference respectively
u	a d -dimensional state (or phase) vector used to represent a primal state
s	set of parameters
$\varphi_s^t(u)$	primal state vector at time t when starting at initial state u , obtained using the parameterized transformation φ_s^t

*Ph.D. Candidate, Department of Mechanical Engineering, nishac@mit.edu, AIAA Student Member

†Ph.D. Candidate, Department of Aeronautics and Astronautics, pablof@mit.edu, AIAA Student Member

‡Developer technology engineer

§Associate Professor, Department of Aeronautics and Astronautics, qiqi@mit.edu, AIAA Associate Fellow

$J(u)$	objective function of interest
$u(t)$	this notation is used to represent the primal state when the initial state need not be explicitly mentioned; note that $\varphi_s^t(u(0)) = u(t)$
$y(t; u)$	adjoint solution at time t corresponding to primal solution starting at initial condition u
$v(t; u)$	tangent solution at time t corresponding to primal solution starting at initial condition u
$f_s(u)$	the vector field on the right hand side of the primal set of ODEs
Dg	the derivative of a scalar or a vector field g wrt to the state; $Dg [u]$ denotes its value at u
$\frac{\partial g}{\partial s}$	partial derivative with respect to s , of a scalar or a vector field g , at the reference value of s ; $\frac{\partial g}{\partial s} [u]$ denotes its value at u
μ_s	stationary measure the statistics wrt which we are interested in
$\mu_s[J]$	phase-space average, according to μ_s , of the function J
$b(\tau)$	bias in $\theta_{\tau, N}$
$\text{var}(\tau, N)$ or $\text{var}(\theta_{\tau, N})$	variance of $\theta_{\tau, N}$
λ_1	largest Lyapunov exponent
γ_1	rate of exponential decay of $b(\tau)$
$f(x) \sim \mathcal{O}(g(x))$	indicates that a function f is on the same order as g . That is, there exists an $x^* \geq 0$ such that $ f(x) \leq C g(x) $, for all $ x \geq x^*$, with the constant $C > 0$ being independent of x .

I. Introduction

GRADIENT-based computational approaches in multi-disciplinary design and optimization (MDO) require sensitivity information computed from numerical simulations of fluid flow. In Reynolds-averaged-Navier-Stokes (RANS) simulations, sensitivity computation is traditionally performed using tangent or adjoint equations or using finite difference methods. Sensitivities computed from RANS simulations have been extensively applied towards uncertainty quantification, mesh adaptation and other MDO applications [1, 2]. Many modern applications require computing sensitivities in direct numerical simulations (DNS) or large-eddy simulations (LES); examples include buffet prediction in high-maneuverability aircraft, modern turbomachinery design and jet engine and airframe noise control. Conventional

tangent/adjoint approaches cannot be used to compute sensitivities of average quantities in these high-fidelity, eddy-resolving simulations. This is because the tangent and adjoint solutions computed from these simulations diverge exponentially [3, 4], since they exhibit chaotic behavior i.e., infinitesimal perturbations to initial conditions grow exponentially in time.

One of the first approaches to circumvent the problem of exponentially diverging linearized perturbation solutions (such as tangent/adjoint) to compute bounded sensitivities is the Lea-Allen-Haine ensemble sensitivity (ES) method [4]. The method approximates Ruelle’s response formula [5] for sensitivity of average quantities to system parameters. It uses a sample average of a finite number of independent tangent or adjoint equation solutions each of which is computed over independent trajectories of short time durations. The convergence of the method has been shown by Eyink et al [6] in the limit of taking an infinite number of samples and increasing the trajectory length to infinity, in that order. Eyink et al [6] establish that the rate of convergence is worse than a typical Monte-Carlo simulation (in which the error in a sample average diminishes at the rate $1/\sqrt{N}$, where N is the number of samples) in the case of the classical 3-variable Lorenz’63 system. However, the convergence trend is still unknown for general chaotic systems. In this work, we present an analysis of the mean squared error of the ES method as a function of the computational cost for a certain class of systems called uniformly hyperbolic systems [7]. It is worth noting that at the time of writing of this paper, alternatives to the ES method [8, 9] are under active investigation. Non-intrusive least squares shadowing (NILSS) [3, 10] and its adjoint-variant [8] are methods that are conceptually based on the shadowing property of uniformly hyperbolic systems. This property enables the computation of a particular tangent solution that remains bounded in a long time window and sensitivities are estimated using this tangent solution. The NILSS algorithm requires the knowledge of the unstable subspace (of the tangent space, corresponding to the positive Lyapunov exponents). This makes the algorithm expensive when the dimension of the subspace or the number of positive Lyapunov exponents is large. The NILSS method has been applied to LES of turbulent flows around bluff bodies [11] at low Reynolds numbers, where the number of positive Lyapunov exponents is small enough to limit the computational expense when compared to wall-bounded flows, for instance.

The paper is organized as follows. In the next section, we review the ES method and define the ES estimator for the sensitivity. In section III, we describe the mean squared error in the ES estimator in terms of the associated bias and variance and obtain optimistic, problem-dependent estimates for both components. We predict the rate of convergence as a function of computational cost under these optimistic assumptions on the dynamics. The rest of the paper consists of numerical examples that illustrate the convergence trend of the ES method. In sections IV.A and IV.B, we discuss two low-dimensional models of chaotic fluid behavior: the Lorenz’63 and Lorenz’96 systems. We apply our optimistic analysis to roughly estimate an upper bound on the rate of convergence. We then present two numerical simulation results that serve to illustrate the applicability of ES schemes in fluid simulations of practical interest, in light of our mathematical analysis in section III. The first is a simulation of a NACA 0012 airfoil in section IV.C and the second, an

LES of turbulent flow around a turbine vane in section IV.D.

II. The ES estimator

A. The sensitivity computation problem setup

Consider a chaotic fluid flow parameterized by s , expressed through an ODE of the following form:

$$\frac{d\varphi_s^t(u)}{dt} = f_s(\varphi_s^t(u)) \quad u \in \mathbb{R}^d, s \in \mathbb{R}^p. \quad (1)$$

Here, we use $\varphi_s^t(u)$ to denote the state vector at time t obtained due to the evolution of an initial state u according to equation 1. As an example, if equation 1 is the spatially discretized incompressible Navier-Stokes equation, a state vector consists of the velocity components, pressure and temperature at all the grid points. Then, φ_s is the parameterized spatially-discretized Navier-Stokes operator and $d = 5 \times$ the number of degrees of freedom. If $u \in \mathbb{R}^d$ is the initial flow field, $\varphi_s^t(u) \in \mathbb{R}^d$ represents the flow field at time t . $\varphi_s^t(u)$ is approximately known from numerical simulation and can be thought of as a point in the phase space M , a compact subset of \mathbb{R}^d . The set of input parameters s can be, for instance, related to the inlet conditions, the geometry of the domain or solid bodies in the flow and so on. In the interest of simplicity, from here on, s is a scalar parameter.

The fluid flows we consider here are statistically stationary, i.e., the states in phase space are distributed according to a time-invariant probability distribution μ_s . The subscript s indicates that the stationary distribution is a function of the parameter; we work under the assumption that μ_s is a smooth function of s . Suppose J is a smooth scalar function of the state such as the lift/drag ratio or the pressure loss in a turbine wake. The mean of J is defined as its expectation with respect to μ_s and denoted by $\mu_s[J] := \int J d\mu_s$. We are interested in computing the sensitivity of $\mu_s[J]$ to s . The phase space average, $\mu_s[J]$, can be measured as a time average along almost every trajectory, under the assumption of ergodicity. More precisely, for almost every initial state u ,

$$\mu_s[J] = \lim_{t \rightarrow \infty} \frac{1}{t} \int_0^t J(\varphi_s^{t'}(u)) dt'.$$

In practice, $\mu_s[J]$ is computed approximately as a finite-time average by truncating a trajectory at a large t . The Lea-Allen-Haine ES method, the subject of this paper, computes the sensitivity $d_s \mu_s[J]$ approximately, as we describe next.

B. The Lea-Allen-Haine ES algorithm

The ES estimator of the sensitivity is the sample mean of a finite number of independent sensitivity outputs computed over short trajectories. We now make this statement precise in the following description of the ES algorithm. Consider

N independent initial states $\{u_0^{(i)}\}_{i=1}^N$, sampled according to μ_s . Let us denote the sensitivity computed along a flow trajectory, of length τ , starting from $u_0^{(i)}$, as $\theta_\tau^{(i)}$. Then, the Lea-Allen-Haine estimator $\theta_{\tau,N}$, is given by,

$$\theta_{\tau,N} = \frac{1}{N} \sum_{i=1}^N \theta_\tau^{(i)}. \quad (2)$$

The standard adjoint method was proposed to be used originally [4, 6] to compute the sensitivities $\theta_\tau^{(i)}$ in order to retain the advantage of adjoint methods, namely that their computational cost does not increase with the dimension of the parameter space. The analysis in the remainder of this paper would be identical however, if the tangent equation or a finite difference approximation to the sensitivity derivative was used instead. The three methods of computing $\theta_\tau^{(i)}$, dropping the superscript i for clarity, are listed below. The sensitivity estimator computed using Eq. 2 when $\theta_\tau^{(i)}$ are computed using the tangent equation, adjoint equation and from finite difference are denoted using $\theta_{\tau,N}^T$, $\theta_{\tau,N}^A$ and $\theta_{\tau,N}^{FD}$ respectively.

1) From the tangent equation:

$$\frac{dv(t; u_0)}{dt} = \frac{\partial f_s}{\partial s} [\varphi_s^t(u_0)] + Df_s [\varphi_s^t(u_0)] v(t; u_0) \quad (3)$$

where, $v(t; u_0) = (d\varphi_s^t(u_0)/ds)$ is the tangent solution at time t when the primal initial condition is u_0 . The tangent initial condition $v(0; u_0) = 0 \in \mathbb{R}^d$ since u_0 is independent of s . We use the symbol $Dg[u]$ to represent the gradient of a function g evaluated at a phase point $u \in \mathbb{R}^d$. So, $Df_s [\varphi_s^t(u_0)]$ is the Jacobian matrix of the vector field f_s at the time instant t for an initial condition u_0 . Then, we have,

$$\theta_{\tau,N}^T = \frac{1}{\tau N} \sum_{i=1}^N \int_0^\tau DJ [\varphi_s^t(u_0^{(i)})] \cdot v(t; u_0^{(i)}) dt. \quad (4)$$

2) From the adjoint equation:

$$\frac{dy(t; u_0)}{dt} = -DJ [\varphi_s^t(u_0)] - (Df_s)^* [\varphi_s^t(u_0)] y(t; u_0), \quad (5)$$

where $y(\tau; u_0) = 0 \in \mathbb{R}^d$ is the adjoint vector at time τ which results in the adjoint vector $y(t; u_0)$ at time t when evolved backwards in time for a time $\tau - t$. $(Df_s)^* [\varphi_s^t(u_0)]$ is the adjoint of the Jacobian at time t for the primal initial condition u_0 .

Then, we have,

$$\theta_{\tau,N}^A = \frac{1}{\tau N} \sum_{i=1}^N \int_0^\tau y(t; u_0^{(i)}) \cdot \frac{\partial f_s}{\partial s} [\varphi_s^t(u_0^{(i)})] dt. \quad (6)$$

3) Using a finite difference approximation:

$$\theta_{\tau,N}^{\text{FD}} = \frac{1}{\tau N} \sum_{i=1}^N \frac{1}{2\Delta s} \left(\int_0^\tau J \circ \varphi_{s+\Delta s}^t(u_0^{(i)}) dt - \int_0^\tau J \circ \varphi_{s-\Delta s}^t(u_0^{(i)}) dt \right), \quad (7)$$

for a small Δs .

III. Error vs. computational cost of the ES estimator

Chaotic systems such as turbulent fluid flows often exhibit regularity in long-time averages despite showing seeming randomness in instantaneous measurements. The chaotic hypothesis, proposed by Gallavotti and Cohen [12], is the notion that these systems can be treated, for the purpose of studying their long-time behavior, as having a certain smooth structure in phase space. This smooth structure allows for the existence of subspaces of the tangent space consisting of expanding and contracting derivatives of state functions. Our goal in this section is to predict the convergence trend of the ES method for systems that satisfy the chaotic hypothesis. More specifically, we would like to construct an optimistic model for the least mean squared error of the ES method, achievable for a given computational cost, in these systems. Before we delve into the construction of the optimistic model, we will discuss the rigorous justification for the convergence of the ES method - Ruelle's response formula. Here we will focus on the implications of the formula for the ES method without going into details; the reader is referred to Ruelle's original paper [5, 13] for the derivation of the response formula. We shall refrain from a technical discussion on hyperbolicity and other concepts from dynamical systems theory but provide the necessary qualitative description, in the context used here.

A. ES estimator as approximation of Ruelle's response formula

The following response formula [14] due to Ruelle gives the sensitivity of the statistical average of the objective function J to a perturbation in s :

$$\frac{d\mu_s[J]}{ds} = \int_0^\infty dt \int_M D(J \circ \varphi_s^t)[u] \cdot \frac{\partial f_s}{\partial s}[u] d\mu_s(u). \quad (8)$$

One can interpret the inner integral (over M) as the statistical response of the objective function at time instant t . It is a phase space average of the sensitivity at time t with the initial conditions distributed according to the stationary probability distribution μ_s . Ruelle's formula has been proven to hold for a certain class of smooth dynamical systems known as uniformly hyperbolic systems. Roughly speaking, these are systems in which the tangent space at every point in phase space can be split into stable and unstable subspaces, which contain respectively, exponentially decaying and growing tangent vectors. In reality, the formula is applicable to a large class of fluid flow problems (this wider applicability referenced earlier as the chaotic hypothesis) that are not necessarily uniformly hyperbolic, as subsequent works [5, 12] have analyzed.

An iterated integral such as in equation 8, gives the same value upon switching the order of integration if and only if the double integral in which the integrand is replaced by its absolute value, is finite (this is the Fubini-Tonelli theorem). The absolute value of the integrand in equation 8 diverges to infinity as $t \rightarrow \infty$ for almost every initial condition in phase space. More precisely, in a chaotic system, for every initial condition u in phase space except those in a set of μ_s -measure 0,

$$\int_0^\infty \left| D(J \circ \varphi_s^t)[u] \cdot \frac{\partial f_s}{\partial s}[u] \right| dt = \infty.$$

For this reason, in 8, the integral over phase space and over time do not commute. The iterated integral in 8 in which the integration over phase space is performed first, leads to a bounded value, which is equal to $d\mu_s[J]/ds$. On the other hand, changing the order of integration and integrating over t first, results in infinity.

From here on, we use the following approximation as the definition of the ES estimator

$$\theta_{\tau,N} := \frac{1}{N} \sum_{i=1}^N \int_0^\tau D(J \circ \varphi_s^t)[u_0^{(i)}] \cdot \frac{\partial f_s}{\partial s}[u_0^{(i)}] dt, \quad (9)$$

where the set of initial states $\{u_0^{(i)}\}_{i=1}^N$ are independent and identically distributed according to μ_s . The ES estimator can be interpreted as an approximation of Ruelle's formula in the following sense: if the outer integral over time (in equation 8) is truncated at time τ and the phase space average of the integrand approximated with a sample mean over N independent samples, we obtain the estimator in equation 9. The definition can also be interpreted as the sensitivity of $\int_0^\tau J \circ \varphi_s^t(u_0) dt$ to s computed using the method outlined in section II.B but using the homogeneous tangent equation. That is, consider the tangent equation 3 without the source term $(\partial f_s / \partial s)[\varphi_s^t(u_0)]$ solved with the initial condition $v(0; u_0) = (\partial f_s / \partial s)[u_0]$. Then, the solution of equation 3 at time t is given by

$$v(t; u_0) = D\varphi_s^t[u_0] \frac{\partial f_s}{\partial s}[u_0].$$

Therefore, the sensitivity of $\int_0^\tau J \circ \varphi_s^t(u_0) dt$ with respect to s is obtained using,

$$\frac{\partial}{\partial s} \int_0^\tau J \circ \varphi_s^t(u_0) dt = \int_0^\tau DJ[\varphi_s^t(u_0)] v(t; u_0) dt = \int_0^\tau D(J \circ \varphi_s^t)[u_0] \cdot \frac{\partial f_s}{\partial s}[u_0] dt.$$

Taking an N -sample average of the above results in the formula for the estimator 9. The resulting $\theta_{\tau,N}$ is different from the sensitivities $\theta_{\tau,N}^{\text{FD}}$, $\theta_{\tau,N}^{\text{T}}$ and $\theta_{\tau,N}^{\text{A}}$ defined in section II.B, all of which are also different from one another. However, in the asymptotic limit of $\tau \rightarrow \infty$, all these sensitivities grow exponentially at the same rate determined by the largest among the Lyapunov exponents (the asymptotic exponential growth or decay rate of tangent/adjoint vectors) of the system. Therefore, for the purpose of an asymptotic analysis, we restrict our attention to the estimator defined by equation 9 and refer to $\theta_{\tau,N}$ using the umbrella term ES estimator.

One notices that in the practical computation of the ES method, the integrals are commuted when compared to Ruelle’s formula but the integral in time is truncated at a finite time. As noted in Eyink et al’s analysis [6], the rationale behind swapping the order of integration as compared to Ruelle’s formula in equation 8 is the observation that the “divergence of the individual adjoints is delayed on taking a sample average”, for the Lorenz’63 system, a low-order model for fluid convection that we discuss in section IV.A. In the rest of the paper, our goal is to analyze the convergence trend in more generality.

B. Bias and variance of the ES estimator

Having defined the ES estimator, we now construct an optimistic model for its mean squared error in uniformly hyperbolic systems. In this section, we present our choice of optimistic estimates for the bias and the variance associated with the estimator and use uniform hyperbolicity to justify our choices. The ES estimator, as defined in 9, has a non-zero bias for a finite τ . By definition, the bias, denoted by $b(\tau)$, gives the difference between the value attained by the estimator on using an infinite number of samples and the true value of the sensitivity,

$$b(\tau) = \mu_s[\theta_{\tau,N}] - \frac{d\mu_s[J]}{ds}. \quad (10)$$

Therefore b is only a function of τ (and not N) because on using an infinite number of samples,

$$\lim_{N \rightarrow \infty} \theta_{\tau,N} = \mu_s[\theta_{\tau,N}] = \int_M d\mu_s \int_0^\tau D(J \circ \varphi_s^t) \frac{\partial f_s}{\partial s} dt. \quad (11)$$

Writing equation 10 more explicitly as,

$$b(\tau) = \int_M \int_0^\tau D(J \circ \varphi_s^t) \frac{\partial f_s}{\partial s} dt d\mu_s - \int_0^\infty \int_M D(J \circ \varphi_s^t) \frac{\partial f_s}{\partial s} d\mu_s dt, \quad (12)$$

clearly indicates why there is a non-zero bias for a finite value of τ . As an optimistic estimate of $b(\tau)$, we choose an exponential decay at a problem-dependent rate denoted γ_1 , using the following justification. In a uniformly hyperbolic system, a tangent vector can be decomposed, at every point in phase space, into its stable and unstable components. A stable (unstable) tangent vector would diminish in norm along a forward (backward) trajectory at an exponential rate. More precisely, for almost every u_0 , if $v(0; u_0)$ is a stable tangent vector at u_0 , there exist $C, \alpha > 0$ such that,

$$\|v(t; u_0)\| \leq C \exp(-\alpha t) \|v(0; u_0)\|, \quad \text{for all } t \geq 0. \quad (13)$$

That is, in uniformly hyperbolic systems, solving the homogeneous tangent equation with a stable tangent vector as the initial condition, results in a stable tangent vector $v(t)$ whose norm is exponentially smaller than that of $v(0)$. Let us

now examine the bias when the initial perturbation given by $(\partial f_s / \partial s)[u_0]$ is a stable tangent vector at every u_0 . From equation 12,

$$b(\tau) = - \int_M \int_\tau^\infty D(J \circ \varphi_s^t) \frac{\partial f_s}{\partial s} dt d\mu_s \quad (14)$$

$$\begin{aligned} &= - \int_M \int_\tau^\infty (DJ \circ \varphi_s^t) D\varphi_s^t \frac{\partial f_s}{\partial s} dt d\mu_s \\ &= - \int_M DJ \int_\tau^\infty D\varphi_s^t \circ \varphi_s^{-t} \frac{\partial f_s}{\partial s} \circ \varphi_s^{-t} dt d\mu_s \circ \varphi_s^{-t}. \end{aligned} \quad (15)$$

$$\implies |b(\tau)| \leq \frac{C}{\alpha} \|DJ\| \left\| \frac{\partial f_s}{\partial s} \right\| \exp(-\alpha\tau), \quad (16)$$

where the norm $\|\cdot\|$ of a vector field X expressed in coordinates as $X(u) = [X_1(u), X_2(u), \dots, X_d(u)]$ is defined as

$$\|X\| := \left(\sum_{i=1}^d \int_M |X_i|^2 d\mu_s \right)^{1/2}.$$

We obtain equation 14 by recognizing that the order of integration can be swapped in the second term (the true sensitivity) in equation 12 in this case since the absolute value of the integrand is an exponentially decreasing function of time. From equation 14, equation 15 can be obtained by using the fact that an ensemble average of the integrand with respect to μ_s remains unchanged upon moving the time origin from 0 to an arbitrary $t > 0$, since μ_s is a stationary distribution. Equation 16 follows from using Cauchy-Schwarz inequality and the fact that stable perturbations decay in time, as described by inequality 13. Thus, we obtain that the bias of the estimator $\theta_{\tau,N}$ decays exponentially with τ if the perturbations lay entirely in the stable subspace of the tangent space at every point. In general, the initial tangent vector will also have an unstable component. The unstable contribution to the bias follows the decay of time correlations [5] in the system, which has been shown to be exponential, at best, in uniformly hyperbolic systems. Estimating the decay of correlations is an active research area and previous studies [15, 16] have obtained that even among hyperbolic chaotic systems, *intermittent* systems can exhibit subexponential decay of correlations. Therefore, an exponential decay of the bias with integration time is justified as a representation of the optimal scenario, giving rise to the following model for the squared bias, for some constant $C_b > 0$:

$$b^2(\tau) = C_b \exp(-2\gamma_1\tau), \quad (17)$$

where γ_1 is a problem-dependent rate. In the same vein as our discussion on the bias above, we propose a model for the best case variance and provide a justification for the chosen model. The ES estimator $\theta_{\tau,N}$ is a sample average of the random variable $\int_0^\tau D(J \circ \varphi_s^t) (\partial f_s / \partial s) dt$, the randomness arising in the (deterministic) chaotic system due to the randomness in the initial condition. We know that the initial conditions are distributed according to μ_s and this gives

rise to an unknown τ -dependent distribution for $\int_0^\tau D(J \circ \varphi_s^t) (\partial f_s / \partial s) dt$. For a finite τ , we assume that the variance of this distribution is finite. Then, it follows that since $\mu_s[\theta_{\tau,N}]$ is bounded as we established above, the central limit theorem (CLT) applies and therefore, for large N ,

$$\text{var}(\theta_{\tau,N}) \rightarrow \frac{\text{var}(\int_0^\tau D(J \circ \varphi_s^t) (\partial f_s / \partial s) dt)}{N}. \quad (18)$$

The applicability of the CLT for the distribution of $\theta_{\tau,N}$ is in general an optimistic assumption, as discussed in previous works [6] and in the numerical example in section IV.A. It is reasonable to expect that $\text{var}(\int_0^\tau D(J \circ \varphi_s^t) (\partial f_s / \partial s) dt)$ increases exponentially with τ since for almost every initial state, $|D(J \circ \varphi_s^t) (\partial f_s / \partial s)| \sim \mathcal{O}(\exp(\lambda_1 t))$, where λ_1 is called the largest Lyapunov exponent of the system. Therefore, we expect that the variance grows exponentially at the rate of twice the largest Lyapunov exponent of the system. Thus, we propose the following optimistic model for the variance, for some $C_{\text{var}} > 0$,

$$\text{var}(\tau, N) = \frac{C_{\text{var}} \exp(2\lambda_1 \tau)}{N}. \quad (19)$$

C. Optimistic convergence estimate for the ES method

Using the optimistic estimates for the bias and the variance described in section III.B, we arrive at the following ansatz for the mean squared error in the ES estimator:

$$\tilde{e}(\tau, T) = \text{b}^2(\tau) + \text{var}(\tau, N) \quad (20)$$

$$= C_{\text{b}} \exp(-2\gamma_1 \tau) + \frac{C_{\text{var}} \tau}{T} \exp(2\lambda_1 \tau), \quad (21)$$

where we use $T := N\tau$ to denote the computational cost. The relationship between the integration time τ^* that minimizes the mean squared error and the cost T for the model in equation 21 is:

$$\tau^*(T) = \arg \min_{\tau} \tilde{e}(\tau, T) = -\frac{1}{2\lambda_1} + \frac{\mathcal{W}(c)}{2(\gamma_1 + \lambda_1)} \quad (22)$$

where,

$$c = 2 C_{\text{b}} \frac{\gamma_1(\gamma_1 + \lambda_1)T}{C_{\text{var}}\lambda_1} \exp(1 + \gamma_1/\lambda_1)$$

and \mathcal{W} is the Lambert W -function. The above relationship shows that, given constants C_{b} and C_{var} independent of τ , the optimal trajectory length of each independent sensitivity evaluation, τ^* , varies sub-logarithmically with the cost T , as shown in figure 1.

From equations 21 and 22, it can be seen that the least mean squared error, denoted by $\tilde{e}_{\text{min}}(T) := \tilde{e}(\tau^*(T), T)$ can be

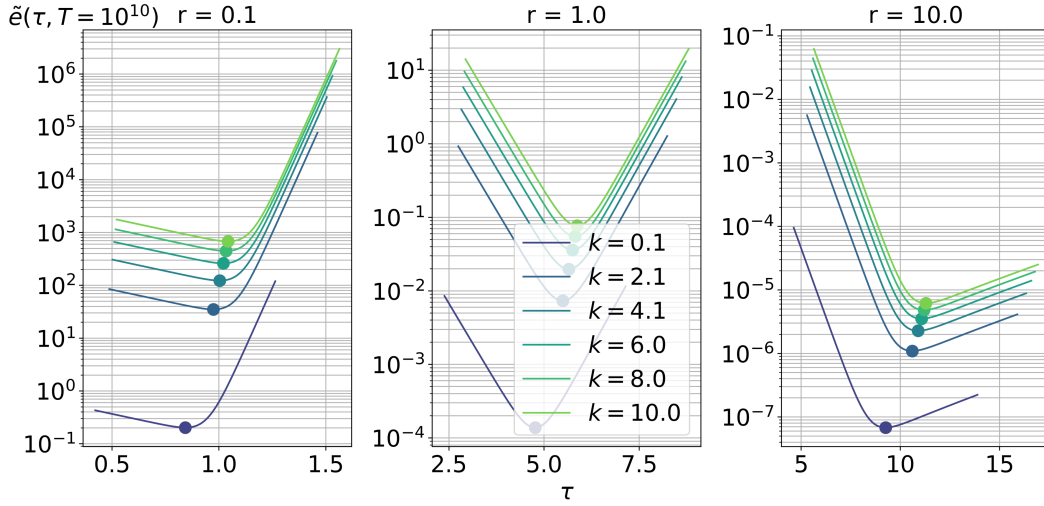
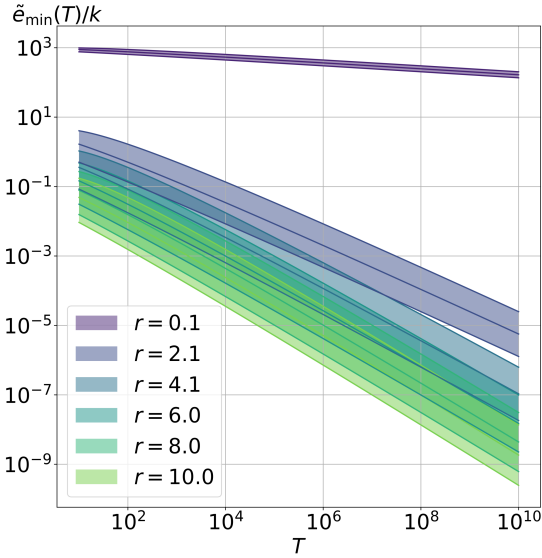


Fig. 1 The mean squared error as a function of integration time τ , for different values of the variables k and r . The optimal value τ^* is marked on each of the plots.

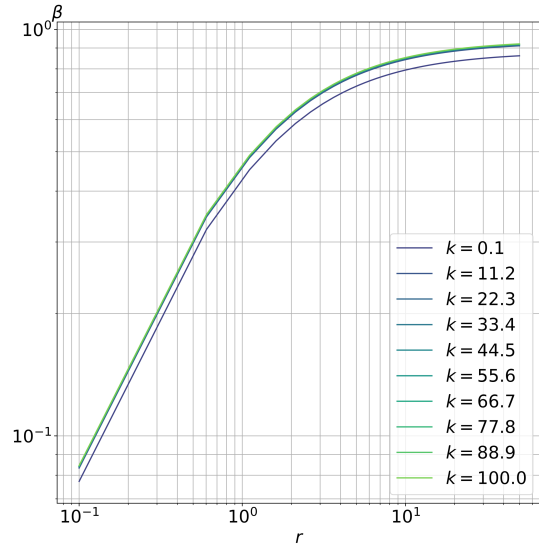
reduced to a function of the variables, $k := C_b\gamma_1/C_{\text{var}}$ and $r := \gamma_1/\lambda_1$. Figure 1 shows the variation of $\tilde{e}(\tau, T)$ with τ at a fixed T , for different values of k and r . In figure 2a, $\tilde{e}_{\min}(T)/k$ is shown against the total computational cost T at different values of r . The plots in figure 2a reveal that \tilde{e}_{\min} is shifted upward on decreasing k but the slope of \tilde{e}_{\min} vs. T , is relatively unaffected by a change in k when compared to a change in r . From figure 2a, we also observe that the least mean squared error \tilde{e}_{\min} decays like an approximate power law of the total cost T . That is,

$$\tilde{e}_{\min} \sim O(T^{-\beta}) \quad \text{for some } \beta \equiv \beta(k, r) > 0. \quad (23)$$

In figure 2b, the rate of convergence β is reported at different values of r and k . From figure 2b, β appears to be quite robust to varying the ratio of the bias to variance coefficients, C_b/C_{var} , when γ_1 is kept constant. On the other hand, it can be seen that the influence of the ratio of timescales r is significant on the rate of convergence. For values of $r > 1$, the least mean squared error falls faster than $1/\sqrt{T}$, for a range of values of k , indicating that convergence rates better than a typical Monte-Carlo sampling can be achieved on choosing an optimal τ under the assumptions of section III.B. This implies that, assuming a strongly chaotic system satisfying our optimistic estimates, when the timescale of the decay of bias is shorter than that of the growth of perturbations ($1/\lambda_1$), the ES method can be very efficient. On the contrary, figure 2b also indicates that the number of samples required to half \tilde{e}_{\min} at $r = 1$ must be increased four-fold while at $r = 0.1$, a factor of 2^{10} increase in the number of samples is required to half the error. To summarize, even in the ideal case of exponential decay of the bias, a rate of decay smaller than the leading Lyapunov exponent, would lead to a significantly less-efficient method than a typical Monte-Carlo.



(a) \tilde{e}_{\min}/k as a function of T , at different values of r .



(b) Rate of convergence as a function of the ratio $r = \gamma_1/\lambda_1$.

IV. Numerical examples

The previous section was dedicated to a mathematical analysis of the convergence of the ES method. We were able to predict the best possible rates of convergence under suitable assumptions on the dynamics. In this section, we treat numerical examples of low-dimensional chaotic systems as well as simulations of turbulent flow. In each of the examples, our goal is to gauge, based on our numerical results, the applicability of the assumptions adopted in our analysis in section III. When deemed applicable, we estimate the rate of convergence using our results from III and discuss the computational tractability of the ES method given this rate. In other cases where either the analysis is inapplicable or the estimation of bias and variance is not practical, we use a physics-informed approach to predict the rate of convergence. The discussions in the following numerical examples delineate guidelines for a priori determination of the practicality of the ES method.

A. The Lorenz'63 attractor

As noted in the introduction, Eyink et al [6] have performed a numerical analysis of the ensemble adjoint and related methods on the Lorenz'63 system and make several important observations regarding the convergence trends of $\theta_{\tau,N}$ in τ and in N . We choose the Lorenz'63 system as the first example in order to validate our present results against Eyink et al's. The Lorenz'63 system is a 3-variable model of fluid convection that is used as a classic example of chaos [17]. It

consists of the following system of ODEs:

$$\begin{aligned}\frac{dx}{dt} &= -\sigma x + \sigma y \\ \frac{dy}{dt} &= -xz + sx - y \\ \frac{dz}{dt} &= xy - bz,\end{aligned}\tag{24}$$

with the standard values of $\sigma = 10$, $b = 8/3$ and $s = 28$. These equations were derived by Lorenz and Saltzman [17] from the conservation equations for a fluid between horizontal plates maintained at a constant temperature difference. The phase vector $u := [x, y, z]^T$, whose evolution these equations describe, corresponds to coefficients in the Fourier series expansion of the stream function and the temperature profile. The parameter s is the Rayleigh coefficient normalized by the critical value above which flow instabilities develop. The objective function of our interest is $J(u(t)) := z(t)$ which is proportional to the deviation of the temperature from the linear profile that would be achieved if the fluid was static. It is well-known that a compact attractor exists in phase space.

We use the algorithms described in section II.B to compute all three types of ES estimators $\theta_{\tau,N}^{\text{FD}}$, $\theta_{\tau,N}^{\text{A}}$ and $\theta_{\tau,N}^{\text{T}}$. To ensure that the initial condition is sampled from the steady-state distribution on the Lorenz attractor, the system is evolved for a spin-off time of about 1.1 time units, before we start computing the sensitivities. This spin-off time is estimated as $1/\lambda_1$, with $\lambda_1 \approx 0.9$ known from the literature to be the largest Lyapunov exponent. The true value of the long-time sensitivity was computed by Eyink et al [6] to be ≈ 0.96 . This value is obtained by numerically computing $\mu_s[J]$ as an ergodic average, at different values of s . It can be seen that $\mu_s[J]$ turns out approximately to be a straight line with a slope of 0.96 for a range of values around $s = 28$. The primal, the tangent and adjoint dynamics in equations 24, 3 and 5 respectively are computed using forward Euler time integration with a timestep of 0.005 time units. The computational cost $T = N\tau$ was chosen to be 5000 time units. The estimators were computed for a range of values of τ up to 3 time units. In order to apply our analysis in section III, we wish to numerically estimate the bias and variance of $\theta_{\tau,N}$. We estimate $\mu_s[\theta_{\tau,N}]$ as a sample average of $\theta_{\tau,N}$ using 5 million independent samples. That is, we approximate $\mu_s[\theta_{\tau,N}]$ as $\theta_{\tau,5 \times 10^6}$ while the true value is not a function of the number of samples but only of τ . The variance of $\theta_{\tau,N}$ is again approximated as a sample average wherein $\mu_s[\theta_{\tau,N}]$ is replaced with its estimate $\theta_{\tau,5 \times 10^6}$.

1. The probability distribution of $\theta_{\tau,N}$

The results from our numerical estimates for the bias and variance of the estimators $\theta_{\tau,N}^{\text{A}}$, $\theta_{\tau,N}^{\text{T}}$ and $\theta_{\tau,N}^{\text{FD}}$, computed as described above, are shown in figure 3a. In figure 3b, the numerical estimates of $\mu_s[\theta_{\tau,N}^2]$ are shown for all three estimators. Before we begin to interpret our numerical results, we briefly describe what we would expect based on Eyink et al's [6] previous work. Their conjecture is that the probability distribution of $\theta_{\tau,N}$ for the Lorenz'63 system is a fat-tailed distribution and does not obey the classical CLT. The underlying implication would be that our assumption

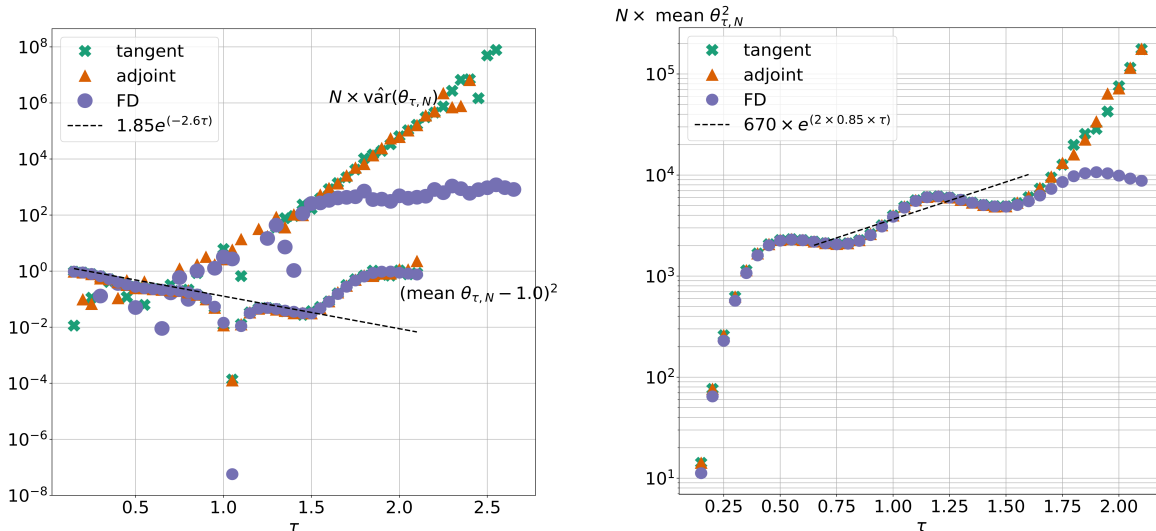
of bounded variance of $\theta_{\tau,N}$ for finite values of τ fails for this system. This represents a fundamental difference between the distribution of sample averages of state functions and that of $\theta_{\tau,N}$, which is a sample average of the instantaneous derivative of a state function. The former distribution has bounded variance but the latter is not guaranteed to. In fact, it has been shown [18] that N -sample averages (computed numerically as ergodic averages) of state functions converge at the rate of $1/\sqrt{N}$. However, the behavior of the N -sample average that $\theta_{\tau,N}$ is, is unlike that of state functions. $\theta_{\tau,N}$ converges to $\mu_s[\theta_{\tau,N}]$ (due to the law of large numbers) at a rate slower than $1/\sqrt{N}$. This rate decreases as τ increases. This bears on the poor accuracy of the estimate $\theta_{\tau,5 \times 10^6}$ for values of $\tau \gtrsim 1.5$ seen in figure 3a, despite using a seemingly large number of samples.

Another observation that can be made from figure 3a is that unlike the variances of $\theta_{\tau,N}^A$ and $\theta_{\tau,N}^T$, $\text{var}(\theta_{\tau,N}^{\text{FD}})$ appears to saturate for $\tau \gtrsim 1.5$. This is explained by the fact that $|\theta_{\tau,N}^{\text{FD}}|$ is bounded above by $\sup(|J|)/\epsilon = c/\epsilon$, where ϵ is the value of the parameter perturbation in the finite difference approximation. The value c is the supremum of the z coordinate of the Lorenz attractor, which is a finite value since the attractor is a bounded set. The fact that $\theta_{\tau,N}^{\text{FD}}$ is bounded for all τ can also be observed in the saturation of the estimate of $\mu_s[\theta_{\tau,N}^{\text{FD}^2}]$ shown in figure 3b.

2. Empirical determination of rate of convergence

Our overarching goal is to predict the rate of convergence of the ES method. We now discuss that it is possible to roughly estimate the rate based on the results we have obtained at a fixed computational cost T . Ignoring transient behavior for τ upto ~ 0.5 , the asymptotic rate of the exponential increase of the estimate of the variance (from figure 3a), is larger than the $2\lambda_1$ rate that we predicted in III.C. To understand this result, let us assert that our estimate of the variance reflects the trend of the true variance and the CLT holds for the given range of values of τ . If the first assertion holds, the true variance is increasing exponentially at a faster rate than $2\lambda_1$. Now, owing to the convergence of Ruelle's formula, we know that $\mu_s[\theta_{\tau,N}]$ cannot have unbounded growth as a function of τ and therefore, the rate of increase of $\text{var}(\theta_{\tau,N})$ must be captured by that of $\mu_s[\theta_{\tau,N}^2]$. From figure 3b, we see that the numerical estimate of $\mu_s[\theta_{\tau,N}^2]$ is indeed exponential in τ at the rate $\sim 2 \times 0.85$ for both the tangent and adjoint estimators, this value of the rate being closer to our theoretical prediction of $2\lambda_1$. Therefore, it is reasonable to conclude that neither of the assertions holds true. As a result, we have considerable error in our estimates of $\mu_s[\theta_{\tau,N}]$ and $\mu_s[\theta_{\tau,N}^2]$ since the error is decaying slower than expected from CLT. Since both these errors play a role in the variance estimation, obtaining the rate of increase from the estimate of $\mu_s[\theta_{\tau,N}^2]$ is more accurate. It is thus reasonable to take the better numerical estimate, 2×0.85 , as the rate of exponential increase of the variance for τ up to 1.5.

In Lea-Allen-Haine's application of the ES method on the Lorenz'63 system [4], $\tau = 1$ is used to obtain an accurate estimate of $d\mu_s[J]/ds$. Our numerical results indicate that both the variance and bias trends are worse than our optimistic model. Therefore, locally around $\tau \sim 1$, operating under the assumption that the bias and the variance trends can be empirically modelled using our optimistic estimates, will provide an upper bound on the actual convergence rate. The



(a) Estimates of the variance and the bias of $\theta_{\tau,N}$ as a function of τ , for the Lorenz'63 system outlined in section IV.A. (b) Sample mean estimates of $\mu_s[\theta_{\tau,N}^2]$ as a function of τ for the Lorenz'63 system outlined in section IV.A.

parameters of the optimistic model estimates of III.B are the local slopes obtained from results in figures 3b and 3a. As noted earlier, for values of $\tau \leq 1.5$, our numerical results indicate that for $\lambda_1 = 0.85$, the rate of increase of the variance can be modelled as $C_{\text{var}} \exp(2\lambda_1 \tau)/N$. Furthermore, the bias does appear to be converging exponentially at the rate $\gamma_1 \sim 1.3$, for $\tau \leq 1.5$, as shown in figure 3a. Therefore, we obtain $r = 1.5$ as the rough estimate needed to determine the rate of convergence under our model assumptions in sec III.C. Thus, we note from figure 2b that $\beta \sim 0.4$. It would not be gainful to also estimate k since we only sought an upper bound for β which is quite insensitive to k , in the first place. We can interpret this rate as the best possible rate of convergence for the Lorenz'63 system. Owing to the fact that $\tau \sim 1$ is not large enough for the failure of the CLT assumption to be manifest, our empirically determined rate from the model agrees well with that estimated using Eyink et al's tail estimates. Thus we conclude firstly that our numerical results provide further evidence in support of the failure of the CLT for $\theta_{\tau,N}$. Secondly, empirical determination of the optimistic rate of convergence under the CLT assumption locally around $\tau \sim 1$, predicts a convergence slower than a Monte-Carlo simulation, confirming Eyink et al's observations.

B. The Lorenz'96 model

Our results for the Lorenz'63 system in section IV.A show that the rate of convergence for an optimal choice of τ (~ 1) is about 0.4. Although this rate is slower than a typical Monte-Carlo simulation, one can immediately see that since the system is low-dimensional, ES is still practical in the Lorenz'63 system. In this section, we aim to assess the computational practicality of the ES method in a higher-dimensional system. We consider the atmospheric convection model, called the Lorenz'96 [19] model, that is known to have a strange attractor [20]. The 40-dimensional state vector

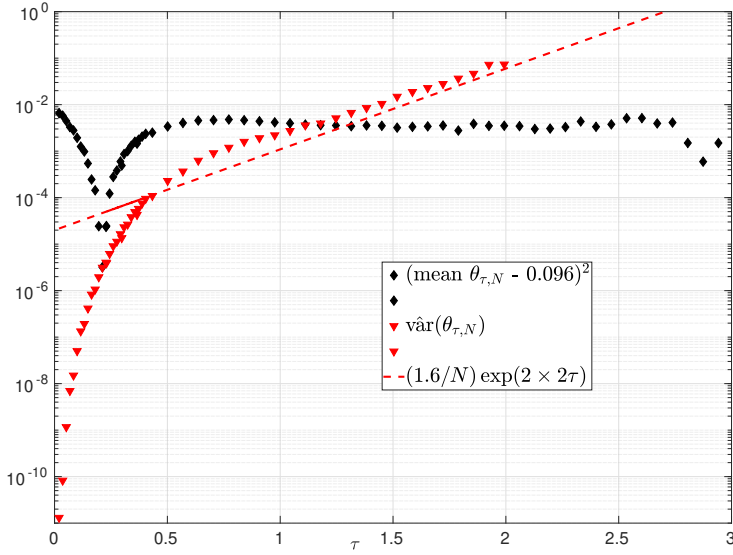


Fig. 4 The variance and the square of the bias in the ensemble tangent sensitivity estimator for the Lorenz'96 system.

$u := [x_1, \dots, x_{40}]^T$ evolves according to the following set of odes [19, 20]

$$\frac{dx_k}{dt} = (x_{k+1} - x_{k-2})x_{k-1} - x_k + s, \quad k = 1, \dots, 40, \quad (25)$$

where, s , the parameter of interest, denotes an external driving force. The first term on the right hand side of equation 25 represents non-linear advection and the second term represents a viscous damping force. Together, the advection and damping terms conserve the kinetic energy of the system, given by $\|u\|^2$. The components of the state vector are periodic in the sense that $x_k = x_{40+k}$, $k \in \mathbb{N}$. We define our objective function $J(u(t))$ to be the mean of the components of u , i.e.,

$$J(u(t)) = (1/40) \sum_{k=1}^{40} x_k(t).$$

We use the value $s = 8.0$ for the forcing term, at which the system has been shown to exhibit chaotic behavior [20]. Time integration of the equations 25 of the primal system is performed using a fourth order Runge-Kutta scheme with a timestep of 0.01 time units. The distribution of each component of the state vector for this system is known from the literature [21] to converge to a Gaussian and the mean state J approximately becomes a linearly varying function with s , on long-time evolution. The slope of $\mu_s[J]$ vs. s estimated from our computations and previous work [20] is 0.096.

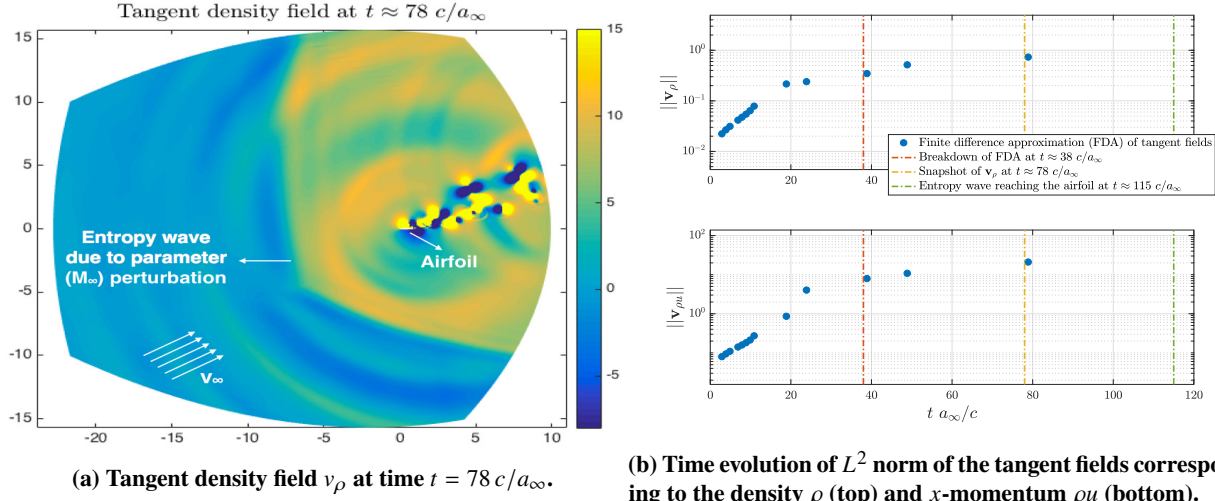
In figure 4, we report the squared bias and the variance of the estimator $\theta_{\tau,N}^T$ as a function of τ . The total cost $T = 10^4$ time units across different values of τ . The values of $\mu_s[\theta_{\tau,N}]$ and $\mu_s[\theta_{\tau,N}^2]$ are computed as sample means and used in the approximation of the bias and variance (denoted by $\hat{\text{var}}(\theta_{\tau,N})$ in figure 4 to indicate the approximation as a

sample mean) terms, identical to our description in section IV.A for the Lorenz'63 system. From figure 4, we can see that the variance follows our model assumptions in section III.B; we find that the variance is exponential in τ at the rate ≈ 4 , which is close to twice the leading Lyapunov exponent reported in the literature [20, 21]. From figure 4, ignoring initial transients, it can be seen that the bias term does not show an exponential convergence, not even locally in the vicinity of $1/\lambda_1 \approx 0.5$. As a result, our local analysis to produce a rough estimate under our model assumptions, as we did in section IV.A, is not applicable in this case. This necessarily implies that the rate of convergence is worse than our model in III.B (for any r) since the bias falls slower than the assumed exponential. One can argue that the mean squared error (sum of the squared bias and the variance) is low in absolute value for τ near 0.5 deeming the ES estimator to be reasonably accurate and therefore practically applicable, although the rate of convergence on increasing the value of τ may be low. However, note that the rate of convergence is an objective function-independent measure of the ES estimator while the mean squared error is not - the latter quantity may be coincidentally within required accuracy for a choice of τ , for this particular objective function. Thus, it is reasonable to conclude that the ES method is infeasible for the Lorenz'96 model.

C. Chaotic flow over an airfoil

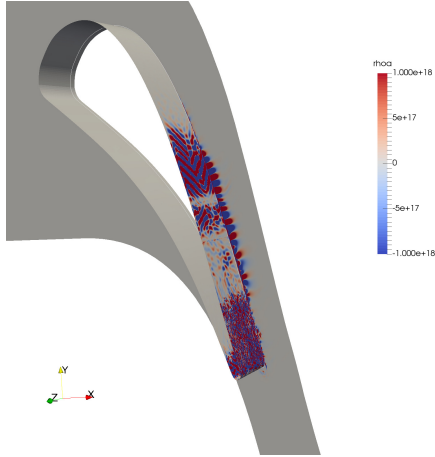
In this example, we discuss the numerical simulation of an unsteady, chaotic flow around a two-dimensional airfoil. So far, we have assessed the convergence of the ES method by observing the trends in the bias and variance of $\theta_{\tau,N}$ in low-dimensional systems. Our numerical results were informative enough to predict the rate of convergence while simultaneously being within the limits of practical computation, owing to the low dimensionality of the systems considered in sections IV.A and IV.B. In contrast, in a typical chaotic CFD simulation, it would not be practical to numerically estimate the bias and variance trends of $\theta_{\tau,N}$. We will thus attempt to predict the convergence trend using a single finite-difference solution (that can be used to compute one sample of $\theta_{\tau,N}$). Our goal is to use a physics-based approach that eliminates the need for a rich $\theta_{\tau,N}$ data set. We consider the NACA 0012 airfoil at the Reynolds number $Re_\infty = 2400$ and Mach number $M_\infty = 0.2$ at an angle of attack $\alpha = 20^\circ$. Although the flow physics in three-dimensional turbulent flows is more complex, the two-dimensional airfoil case we consider exhibits the phenomena of stall and flow separation that are responsible for the chaotic behavior. For an extensive analysis of the Lyapunov spectrum and its dependence on the numerical discretization for this problem, see [22, 23].

The primal system is the set of compressible Navier-Stokes equations, which are discretized in space using a third-order Hybridizable Discontinuous Galerkin (HDG) method [24, 25] with the Friedrichs-Lax-type stabilization matrix in [26]. The computational domain spans $\sim 10 - 20$ chord lengths away from the airfoil and is partitioned using an O-grid with 35280 isoparametric triangular elements. The use of a large computational domain is customary in external aerodynamics to reduce the change in the effective angle of attack induced by the missing vortex upwash. The state vector u is defined to be the set of coefficients in the basis function representation of the density, the components of

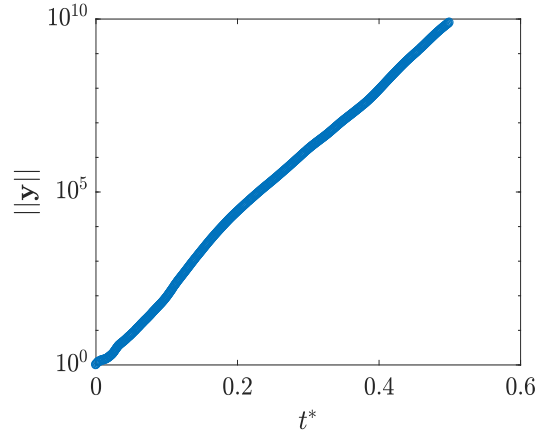


the momenta and the energy, at all elements in the computational domain. Our objective function J is the lift coefficient and the parameter of interest s is the freestream Mach number, M_∞ . A three-stage, third-order diagonally-implicit Runge-Kutta (DIRK) method [27] is used for the temporal discretization. A no-slip, adiabatic wall boundary condition is imposed on the airfoil surface, and the characteristics-based, non-reflecting boundary condition in [24, 25] is used on the outer boundary. The spin-off time before the sensitivity computation is performed is $t = 10,000 c/a_\infty$, where a_∞ denotes the far-field speed of sound and c is the chord length. We note that the chosen spin-off time is one order of magnitude larger than the time required for the convergence of time-averaged flow quantities [22]. At the spin-off time, we reset $t = 0$ and all the results below are indicated with respect to this new initial time.

Since the Jacobian is not available analytically, as is typically the case in CFD codes, the tangent perturbation fields denoted by $v(t)$ are computed non-intrusively with regard to the primal solver using a finite difference approximation (FDA). The parameter perturbation has a magnitude of $\epsilon = 10^{-6}$. Figure 5a shows the sensitivity field of the fluid density with respect to the perturbation in the freestream Mach number at time $t = 78 c/a_\infty$. This quantity, denoted in figure 5b as v_ρ , can be used to compute a single sample of $\theta_{\tau, N}^{\text{FD}}$. The airfoil, much smaller in size than the computational domain, is annotated in figure 5a. Entropy and acoustic waves are generated on the outer boundary at $t = 0$ due to the M_∞ perturbation. From the entropy wavefront shown in figure 5a, one observes that the entropy wave does not reach the airfoil yet at $t = 78 c/a_\infty$. The time evolution of the L^2 norm of the tangent fields corresponding to the density, v_ρ , and the x -momentum, $v_{\rho u}$, are shown in 5b. As we discussed in section IV.A, finite difference sensitivities tend to saturate with time as opposed to tangent and adjoint sensitivities which keep increasing exponentially. This is due to the finite difference sensitivities having an upper bound proportional to $1/\epsilon$, since the supremum of the objective function over phase space is a finite value independent of time. As indicated in figure 5b, the entropy wave reaches the airfoil at $t \sim 115 c/a_\infty$. By this time, the sensitivity fields already saturate. We can estimate by extrapolation that $\|v_\rho\|, \|v_{\rho u}\| > 10^5$ if computed using the tangent equation, at $t = 115 c/a_\infty$.



(a) Adjoint field corresponding to the density, labelled rhoa in the colormap, at $t^* = 0.35$.



(b) The L^2 norm of the adjoint vector field, y , for the Navier-Stokes system in section IV.D as a function of time.

One expects the bias in the ES estimator to be necessarily non-negligible for trajectory lengths shorter than $t = 115 c/a_\infty$. That is, the sensitivities must be computed at least until the time the information about the perturbation propagates to the airfoil, in order for the average sensitivity of the lift to converge to its true value. In other words, convergence of the bias requires the entropy wave to reach the airfoil and thus τ must be larger than $\tau^* := 115 c/a_\infty$. In order to predict the cost of the ES method, let us make the optimistic assumptions that at τ^* , the bias term is close to zero and that the CLT holds for the variance. A random tangent field is at least $\sim 10^5$ in magnitude at τ^* implying that the variance at τ^* would be $O(10^{10})$. Therefore, under the CLT assumption, which we have shown to be too optimistic in our previous examples in sections IV.A and IV.B, one would require on the order of 10^{10} samples for an $O(1)$ mean squared error. Solving the primal and the perturbation equations on the order of 10 billion times for trajectories of lengths τ^* would be computationally infeasible. This example illustrates that constraints imposed by the time scales associated with the flow physics can make the ES method impractical. Here, the constraint is the much shorter time scale of divergence of the adjoint/tangent fields compared to that of the convergence of the bias.

D. Turbulent flow over a turbine vane

As a final example, we consider an implicit LES of turbulent flow around a highly loaded turbine nozzle guide vane performed by Talnikar et al [28]. Our simulations approximate the aero-thermal experimental investigations of turbine guide vanes in a linear cascade arrangement at the von Karman Institute for Fluid Dynamics [29]. The linear cascade is approximated in the simulation domain using periodic boundary conditions in the transverse and spanwise directions. The spanwise extent, is restricted to 0.15 times the chord length c , which has been numerically verified to be sufficient to capture the turbulent flow physics. The Reynolds number of the flow is 10^6 . The isentropic Mach number computed with respect to the static pressure at the outlet is 0.9. Isothermal boundary condition is used on the surface of the vane.

The fluid achieves transonic speeds as it flows over the surface of the vane, transitioning to turbulence on the suction side.

The primal problem is a compressible Navier-Stokes system as in IV.C, solved here using a second order finite volume scheme [28]. A strong stability-preserving third order Runge-Kutta scheme is used for time integration and a weighted essentially non-oscillatory scheme [30] is used for shock capturing. The mesh is generated by uniformly extruding a two-dimensional hybrid structured/unstructured mesh in the spanwise direction.

The long-time averaged objective of interest is the mass-flow averaged pressure loss coefficient on a plane 0.25 chord lengths downstream of the trailing edge of the vane. The reduction in stagnation pressure loss is due to mixing in the turbulent wake and the formation of a boundary layer on the surface of the vane. Sensitivities (computed using the adjoint method) are calculated with respect to Gaussian-shaped source term perturbations to the system dynamics centered 0.3 chord lengths upstream from the leading edge of the vane in the axial direction. The time variable, t^* , is nondimensionalized with respect to the flow-through time, which is the duration of the time taken for fluid flow from the inlet to outlet. In figure 6a, we show the adjoint field corresponding to the density, denoted by ρ_a , at $t^* = 0.35$. Figure 6b shows the L^2 norm of the adjoint field, denoted by y , as a function of t^* . From the growth of the adjoint vectors in figure 6b, we can estimate the leading Lyapunov exponent for the flow to be ~ 46 in nondimensional units. The time taken for the entropy wave of the adjoint solution to reach the source of the perturbation (the propagation direction of the adjoint solution is reversed with respect to the primal flow) is $\gtrsim 0.5$ time units. From figure 6b, we can see that the adjoint solution has diverged by 10 orders of magnitude by this time.

The reason for the rapid divergence is the high angle of attack of the flow onto the vane surface which causes the Mach wave of the adjoint solution to propagate with a maximum speed of Mach 1.9 upstream in the axial direction. The entropy wave, in comparison, has a lower maximum speed of Mach 0.9, which is equal to the flow speed. The adjoint diverges quickly once the Mach wave reaches the turbulent boundary layer region close to the trailing edge of the vane on the suction side, as shown in figure 6a. But the bias in the adjoint computed over an ensemble of trajectories can be expected to decline only for trajectory lengths $\gtrsim 0.5$ time units, which is approximately the time required for the entropy wave to reach the vane leading edge. Similar to the flow over the airfoil presented in section IV.C, the lower speed of propagation of the entropy wave from the inlet makes the ES method infeasible in this problem.

Equipped with the estimate of the Lyapunov exponent and the time scale of convergence of the bias, we predict the cost of the ES method in this case. As in section IV.C, let us assume the best case scenario for both the bias and the variance terms. Suppose the bias has negligible magnitude at 0.5 time units and that the CLT assumption is valid. Since the true variance would be on the order of 10^{20} at $t^* = 0.5$, we would require $O(10^{20})$ samples in order to reduce the variance of $\theta_{0.5,N}^A$ and consequently, the mean squared error to $O(1)$. To roughly estimate the computational power required, we need about 10 teraFLOPS for 12 hours for a single adjoint simulation up to $t^* = 0.5$; this means approximately 10^{15} exaFLOPS for 12 hours would be needed for convergence. This is beyond the computational

capabilities achievable in the near future. To conclude our discussion, even though the source of perturbations is close to the leading edge of the vane, turbulence at a high Reynolds number makes the time scale of the growth of perturbations much shorter than the time required for the propagation of the information about the perturbation through entropy waves. As a result, since the number of samples required for convergence increases exponentially at best with time, the ES method becomes computationally intractable.

V. Conclusion

To compute sensitivities with respect to design parameters, of statistically stationary quantities in chaotic systems, ensemble methods appear to be an appealing solution; they are both conceptually simpler and easier to implement than fluctuation-dissipation-based [9] and shadowing-based [8] methods, all of which are, moreover, still under active development. However, the present work has shown that Eyink et al's [6] results revealing poor convergence of ensemble computations in the Lorenz'63 system, is more widely representative of convergence trends in general chaotic systems. The present work takes the approach of predicting the rate of convergence under the most optimistic assumptions on the system dynamics and demonstrates under these assumptions, a poor rate of convergence, that makes ensemble methods computationally intractable.

The approach is used to perform an analysis of the bias and variance associated with the ensemble sensitivity (ES) estimator, under the mathematical simplification of uniform hyperbolicity. We show that, with the integration time, in the best case, the bias decays exponentially at a problem-dependent rate and the variance increases exponentially at the rate of twice the largest Lyapunov exponent. Assuming these optimistic bounds, the computational cost of the ES method still scales exponentially with the mean squared error. The number of samples required for the ES method to be reasonably accurate is primarily a function of the ratio of the rate of convergence of the bias to the leading Lyapunov exponent of the system.

Our numerical results for the Lorenz'63 system show that the optimistic model proposed for the least mean squared error is locally applicable. The rate of convergence in this case predicted by the error vs. cost analysis in section III concurs with Eyink et al's [6] results; the ES method converges slower than a typical Monte-Carlo simulation for the three variable Lorenz'63 system. The 40-variable Lorenz'96 system serves as an example of a low-dimensional attractor for which the asymptotic convergence is remarkably slow. Although the rate of convergence is poor for this system, the mean squared error magnitudes were low at a reasonable computational cost, for the chosen objective function. This suggests that one may encounter, in practice, objective functions for which the ensemble sensitivities are within a specified accuracy, at an affordable computational cost. In the numerical simulations of chaotic fluid flow we consider, we obtain optimistic estimates on the rate of convergence which hold true for a general objective function. Our results indicate that the flow physics imposes an upper bound on the rate of convergence. Altogether, the present numerical evidence suggests the following: even under the optimistic assumption of exponential decay of the bias, the cost of

exponential sampling of an expensive primal problem makes the ES method infeasible in practical applications.

Funding Sources

This work was supported by AFOSR Award FA9550-15-1-0072 under Dr. Fariba Fahroo and Dr. Jeanluc Cambrier.

Acknowledgments

The authors would like to thank Angxiu Ni for helpful discussions. This research used resources of the Argonne Leadership Computing Facility, which is a DOE Office of Science User Facility supported under Contract DE-AC02-06CH11357. Pablo Fernandez would like to acknowledge financial support from the MIT Zakhartchenko Fellowship.

References

- [1] Peter, J. E., and Dwight, R. P., “Numerical sensitivity analysis for aerodynamic optimization: A survey of approaches,” *Computers & Fluids*, Vol. 39, 2010, pp. 373–391.
- [2] Giles, M. B., and Pierce, N. A., “An introduction to the adjoint approach to design,” *Flow, turbulence and combustion*, Vol. 65, 2000, pp. 393–415.
- [3] Ni, A., and Wang, Q., “Sensitivity analysis on chaotic dynamical systems by Non-Intrusive Least Squares Shadowing (NILSS),” *Journal of Computational Physics*, Vol. 347, 2017, pp. 56–77.
- [4] Lea, D. J., Allen, M. R., and Haine, T. W., “Sensitivity analysis of the climate of a chaotic system,” *Tellus A: Dynamic Meteorology and Oceanography*, Vol. 52, 2000, pp. 523–532.
- [5] Ruelle, D., “Differentiation of SRB states,” *Communications in Mathematical Physics*, Vol. 187, 1997, pp. 227–241.
- [6] Eyink, G., Haine, T., and Lea, D., “Ruelle’s linear response formula, ensemble adjoint schemes and Lévy flights,” *Nonlinearity*, Vol. 17, 2004, p. 1867.
- [7] Katok, A., and Hasselblatt, B., *Introduction to the modern theory of dynamical systems*, Vol. 54, Cambridge university press, 1997.
- [8] Ni, A., “Sensitivity analysis on chaotic dynamical systems by Non-Intrusive Least Squares Adjoint Shadowing (NILSAS),” *arXiv preprint arXiv:1801.08674*, 2018.
- [9] Ragone, F., Lucarini, V., and Lunkeit, F., “A new framework for climate sensitivity and prediction: a modelling perspective,” *Climate Dynamics*, Vol. 46, 2016, pp. 1459–1471.
- [10] Blonigan, P. J., “Adjoint sensitivity analysis of chaotic dynamical systems with non-intrusive least squares shadowing,” *Journal of Computational Physics*, Vol. 348, 2017, pp. 803–826.

- [11] Blonigan, P. J., Fernandez, P., Murman, S. M., Wang, Q., Rigas, G., and Magri, L., “Toward a chaotic adjoint for LES,” *arXiv preprint arXiv:1702.06809*, 2017.
- [12] Gallavotti, G., and Cohen, E., “Dynamical ensembles in stationary states,” *Journal of Statistical Physics*, Vol. 80, 1995, pp. 931–970.
- [13] Ruelle, D., “Differentiation of SRB states: correction and complements,” *Communications in mathematical physics*, Vol. 234, 2003, pp. 185–190.
- [14] Ruelle, D., “Differentiation of SRB states for hyperbolic flows,” *Ergodic Theory and Dynamical Systems*, Vol. 28, 2008, pp. 613–631.
- [15] Baladi, V., Eckmann, J.-P., and Ruelle, D., “Resonances for intermittent systems,” *Nonlinearity*, Vol. 2, 1989, p. 119.
- [16] Baladi, V., *Positive transfer operators and decay of correlations*, Vol. 16, World scientific, 2000.
- [17] Lorenz, E. N., “Deterministic Nonperiodic Flow,” *Journal of Atmospheric Sciences*, 1963.
- [18] Holland, M., and Melbourne, I., “Central limit theorems and invariance principles for Lorenz attractors,” *Journal of the London Mathematical Society*, Vol. 76, 2007, pp. 345–364.
- [19] Lorenz, E. N., “Predictability: A problem partly solved,” *Proc. Seminar on predictability*, Vol. 1, 1996.
- [20] Karimi, A., and Paul, M. R., “Extensive chaos in the Lorenz-96 model,” *Chaos: An Interdisciplinary Journal of Nonlinear Science*, Vol. 20, 2010, p. 043105.
- [21] Venturi, D., Cho, H., and Karniadakis, G. E., “Mori-Zwanzig Approach to Uncertainty Quantification,” *Handbook of Uncertainty Quantification*. Springer, 2016.
- [22] Fernandez, P., and Wang, Q., “Lyapunov spectrum of the separated flow around the NACA 0012 airfoil and its dependence on numerical discretization,” *Journal of Computational Physics*, Vol. 350, 2017, pp. 453–469.
- [23] Pulliam, T. H., and Vastano, J. A., “Transition to Chaos in an Open Unforced 2D Flow,” *Journal of Computational Physics*, Vol. 105, 1993, pp. 133–149.
- [24] Fernandez, P., “Entropy-stable hybridized discontinuous Galerkin methods for large-eddy simulation of transitional and turbulent flows,” Ph.D. thesis, Massachusetts Institute of Technology, 2018.
- [25] Fernandez, P., Nguyen, N., and Peraire, J., “The hybridized Discontinuous Galerkin method for Implicit Large-Eddy Simulation of transitional turbulent flows,” *Journal of Computational Physics*, Vol. 336, 2017, pp. 308–329.
- [26] Fernandez, P., Nguyen, N., and Peraire, J., “Subgrid-scale modeling and implicit numerical dissipation in DG-based Large-Eddy Simulation,” *23rd AIAA Computational Fluid Dynamics Conference*, 2017.

- [27] Alexander, R., “Diagonally implicit Runge–Kutta methods for stiff ODE’s,” *SIAM Journal on Numerical Analysis*, Vol. 14, 1977, pp. 1006–1021.
- [28] Talnikar, C., Wang, Q., and Laskowski, G. M., “Unsteady adjoint of pressure loss for a fundamental transonic turbine vane,” *Journal of Turbomachinery*, Vol. 139, 2017, p. 031001.
- [29] Arts, T., and De Rouvroit, M. L., “Aero-thermal performance of a two dimensional highly loaded transonic turbine nozzle guide vane: A test case for inviscid and viscous flow computations,” *ASME 1990 International Gas Turbine and Aeroengine Congress and Exposition*, American Society of Mechanical Engineers, 1990, pp. V001T01A106–V001T01A106.
- [30] Liu, X.-D., Osher, S., and Chan, T., “Weighted essentially non-oscillatory schemes,” *Journal of computational physics*, Vol. 115, 1994, pp. 200–212.